Optimal matched filter design for ultrasonic NDE of coarse grain materials

Minghui Li and Gordon Hayward

Citation: AIP Conference Proceedings **1706**, 020011 (2016); doi: 10.1063/1.4940457
View online: http://dx.doi.org/10.1063/1.4940457
View Table of Contents: http://scitation.aip.org/content/aip/proceeding/aipcp/1706?ver=pdfcov
Published by the AIP Publishing

Optimal Matched Filter Design for Ultrasonic NDE of Coarse Grain Materials

Minghui Li [1, a)] and Gordon Hayward [2]

[1]*School of Engineering, University of Glasgow, Glasgow G12 8QQ, United Kingdom*
[2]*Centre for Ultrasonic Engineering, University of Strathclyde, Glasgow G1 1XW, United Kingdom*

[a)]Corresponding author: minghui.li@ieee.org

Abstract. Coarse grain materials are widely used in a variety of key industrial sectors like energy, oil and gas, and aerospace due to their attractive properties. However, when these materials are inspected using ultrasound, the flaw echoes are usually contaminated by high-level, correlated grain noise originating from the material microstructures, which is time-invariant and demonstrates similar spectral characteristics as flaw signals. As a result, the reliable inspection of such materials is highly challenging. In this paper, we present a method for reliable ultrasonic non-destructive evaluation (NDE) of coarse grain materials using matched filters, where the filter is designed to approximate and match the unknown defect echoes, and a particle swarm optimization (PSO) paradigm is employed to search for the optimal parameters in the filter response with an objective to maximise the output signal-to-noise ratio (SNR). Experiments with a 128-element 5MHz transducer array on mild steel and INCONEL Alloy 617 samples are conducted, and the results confirm that the SNR of the images is improved by about 10-20 dB if the optimized matched filter is applied to all the A-scan waveforms prior to image formation. Furthermore, the matched filter can be implemented in real-time with low extra computational cost.

INTRODUCTION

Ultrasonic inspection and imaging of coarse grain materials is a challenging yet essential problem which has received considerable attention from the Non-Destructive Evaluation (NDE) community in the recent decades. A variety of coarse grain materials like alloys and stainless steel offer attractive properties like high-temperature strength or excellent resistance to corrosive environment, and thus are widely used to build components like ducting, combustion cans, and transition liner in a range of key industrial sectors such as energy, oil and gas, and aerospace. When these materials are inspected using ultrasound, the flaw echoes are usually contaminated by high-level, correlated noise originating from the microstructure of the tested samples, and the grain noise is time-invariant and demonstrates similar spectral characteristics as flaw signals. A wide variety of techniques have been investigated to suppress grain noise and enhance flaw detection utilizing either the spatial diversity introduced by a transducer array, such as adaptive processing and beamforming [1, 2]; or the temporal-spectral characteristics of the broadband ultrasonic signals, for instance frequency compounding [3], sub-spectrum phase coherence factoring [4], spectral distribution similarity analysis [5], and fragment recognition classification [6].

The signal matching concept has been extensively used in the detection of signals of known form in stationary noise in the application areas like radar and sonar, and more recently in the field of ultrasound NDE. If the signal waveforms and the noise statistics are exactly known *a priori*, the matched filter is optimal in terms of the SNR improvement; this is unfortunately not the case in ultrasonic NDE. Earlier studies utilise point reflector model to design the filter and apply it to clean materials [7], or use flaw signals obtained from simulations to design the filters [8, 9], but they are inevitably subject to errors, especially when using such filters in NDE of coarse grain materials.

In this work, we extend the method for matched filter design in [7] and further develop it into the scenario of inspection of highly scattering materials. The filter is tuned to match the defect echoes which are approximated by the superposition of multiple transmitted signals with different phase shift, time delay and amplitude gain that

42nd Annual Review of Progress in Quantitative Nondestructive Evaluation
AIP Conf. Proc. 1706, 020011-1–020011-9; doi: 10.1063/1.4940457

simulates reflections from an unknown extended target. A particle swarm optimization (PSO) paradigm [10] is employed to search for the optimal parameters in the filter response to maximize the SNR improvements over a set of training signals. Experiments with a 128-element 5MHz transducer array on mild steel and INCONEL Alloy 617 samples are conducted, and the total focusing method (TFM) [1] is used to create the images. The results demonstrate that the SNR of the images is improved by about 10-20 dB when the optimized matched filter is applied to all the A-scan waveforms prior to TFM image formation. The method demonstrates good flaw detection in A-scan waveforms as well even when the SNR is pretty low and the level of grain noise is far above that of flaw echoes. The performance advantages are achieved with low extra computational cost of implementation of the matched filters.

DATA MODEL

If a single point reflector is simulated in a homogeneous and lossless media, the return signal is equal to the transmitted signal except for an unknown time delay and scaling. This simple yet powerful data model is utilised in a variety of literature on radar [11], communications [12, 13], and ultrasonic imaging [14]. However, in most practical NDE applications, the defects are not single or well isolated point reflectors, but are spatially extended and distributed with a spatial profile. A reasonable extension to the data model for a distributed defect is that the defect consists of a number of point-like reflectors, each with given scaling, characteristics and position. The return signal $x(t)$ is then given by a sum of J delayed and scaled versions of the transmitted signal $s_0(t)$,

$$x(t) = \sum_{i=1}^{J} A_i s_0(t - t_i) + n(t), \tag{1}$$

where $s_0(t)$ is the transmitted signal taking into account the excitation waveform and the frequency response of the transducer, J is the number of point-like reflectors under consideration for this particular defect, A_i and t_i are the amplitude and time delay corresponding to a particular point reflector i with certain reflection characteristics and position, and $n(t)$ is the additive noise which is assumed to be uncorrelated with the defect signals.

PROBLEM FORMULATION AND OPTIMAL MATCHED FILTER DESIGN

Assume $x(t)$ to be a return signal from a distributed defect received by a transducer. $x(t)$ is processed by a matched filter with a response $h(t)$ and the output is given by

$$y(t) = x(t) * h(t), \tag{2}$$

where * stands for the convolution operation. $x(t)$ is composed of signal components which is determined by the defect profile and characteristics as well as the additive noise, as illustrated in (1). Based on the theory of matched filtering, if the filter response $h(t)$ is exactly matched to the defect echo, that is

$$h_{opt} = \sum_{i=1}^{J} A_i s_0(t - t_i). \tag{3}$$

the SNR of the output $y(t)$ will be maximised. However, the defect echoes are unknown, and the number of point reflectors J, the delays t_i and the amplitudes A_i are all unknown. The goal of the optimal matched filter design is to tune the parameters of the filter $h(t)$ to approximate the unknown defect echoes and obtain an optimal matched filter, so that the output SNR is maximized for a set of given return signals.

In mathematics, the above-mentioned problem can be formulated by the following equations:

$$\max_{A_i, t_i} \mathrm{SNR}\left[y(t)\right] \quad \text{subject to} \quad \begin{aligned} y(t) &= h(t) * x(t) \\ h(t) &= \sum_{i=1}^{K} A_i s_0(t - t_i) \\ x(t) &= \sum_{i=1}^{J} A_i s_0(t - t_i) + n(t) \end{aligned} \tag{4}$$

where K is the number of point reflectors considered in the approximation, which is unknown *a prior* and is a design parameter. The dependence of the cost function $\mathrm{SNR}\left[y(t)\right]$ on the control variables A_i and t_i is supposed to be non-linear, high-dimensional and complicated, and a numerical optimization paradigm such as the Particle Swarm Optimization is in a good position to tackle this problem. Due to the space constraints, PSO is not discussed in details in this paper, but the readers may refer to [15, 16] and the references therein for more details about design of the PSO routine and selection of the parameters.

EXPERIMENTAL VERIFICATION

The performance of the optimal matched filters designed using the PSO paradigm for ultrasonic NDE imaging and defect detection is demonstrated and analysed in this section. The experimental apparatus consists of the test samples, the ultrasonic transducer array, the phased array control system, and a personal computer. A 128-element transducer array with 0.7 mm element pitch and 5MHz central frequency (Vermon, Tours, France) is utilised in contact with the test sample upper surface with gel coupling, as shown in Fig. 1(a). An OPEN ultrasonic phased array control system with 128 independent parallel channels and 16-bit resolution (LeCouer, Chuelles, France) is connected with the transducer array for excitation and data acquisition, as shown in Fig. 1(b). A personal computer is then connected to the OPEN system to control the excitation sequence and record the return signals for post processing and imaging. A MATLAB (The MathWorks, Natick, MA) routine is developed to implement the Full Matrix Capture (FMC) data acquisition, where each transducer element is excited sequentially and the echoes received by all the array elements are recorded [1]. A complete FMC data set is composed of N^2 A-scan waveforms, where N is the number of array elements. Test samples with different materials and characteristics are employed in the experiments.

The matched filter response is modelled using equation (3) with K reflectors and all the unknown parameters are captured in the particle location vector with a dimension of $2K$. The output SNR is maximised if the filter response is matched to the defect echo, and the parameters are tuned and optimised with the PSO search. The key parameters used in the PSO routine are summarised in Table 1, and the convergence is observed in all the experiments within the maximum number of iterations.

Experiment I

A test sample of a solid mild steel block with a thickness of 60mm is employed in this experiment. There are multiple 3 mm diameter cylindrical side-drilled holes at different lateral positions and depths. The FMC data set is recorded at a sampling rate of 40 MHz, and each A-scan waveform is pre-filtered with a band-pass filer to remove the DC drift and high frequency noise. The mild steel demonstrates homogeneous properties and is less scattering when 5 MHz ultrasound is applied. Fig. 2(a) shows the return signal at Element 68 which is located close to the centre of the array, where the echoes from reflectors like the side drilled holes and the back-wall are significant in comparison to the grain noise, and the SNR is measured to be 18 dB. Fig. 3(a) demonstrates the image obtained with the Total Focusing Method (TFM) [1] using the band-pass filtered FMC data set in a dynamic range of 40 dB. The holes and the back-wall are easily identified and the clutter noise is not significant.

TABLE 1. PSO parameters.

PSO Parameters	Value
K	15
Number of Particles	150
Number of Iterations	500
c_1	0.4
c_2	1.2
Inertia Weight	0.8

(a) (b)

FIGURE 1. Experimental apparatus. (a) Transducer array and test sample, and (b) OPEN phased array control system.

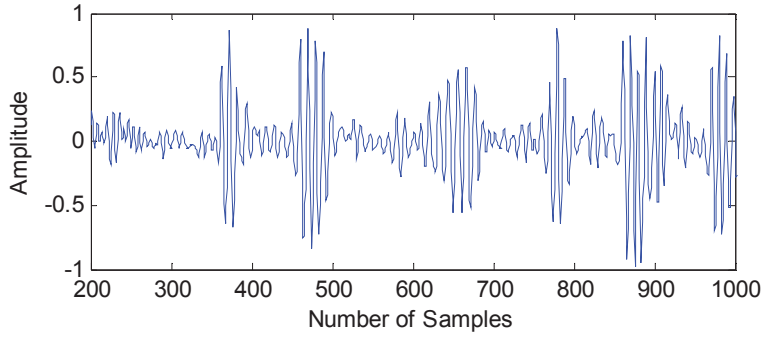

(a)

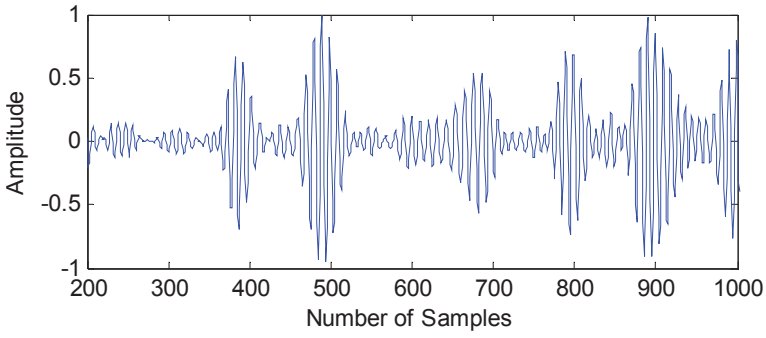

(b)

FIGURE 2. A-scan waveforms at Element 68. (a) Original, and (b) Matched filtered.

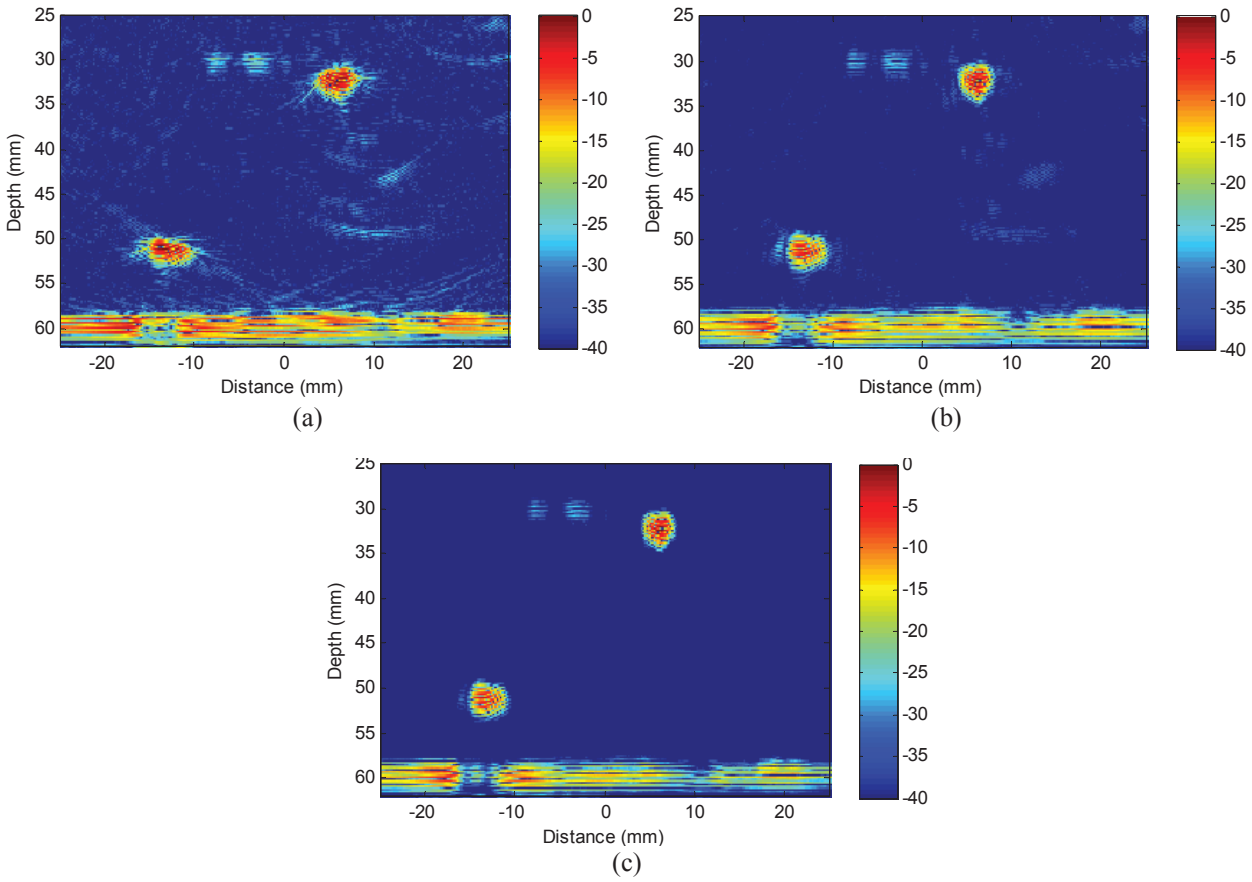

FIGURE 3. Images of mild steel block. (a) TFM with original FMC data set, (b) TFM with matched filtered FMC data set, and (c) Adaptive beamforming with matched filtered FMC data set.

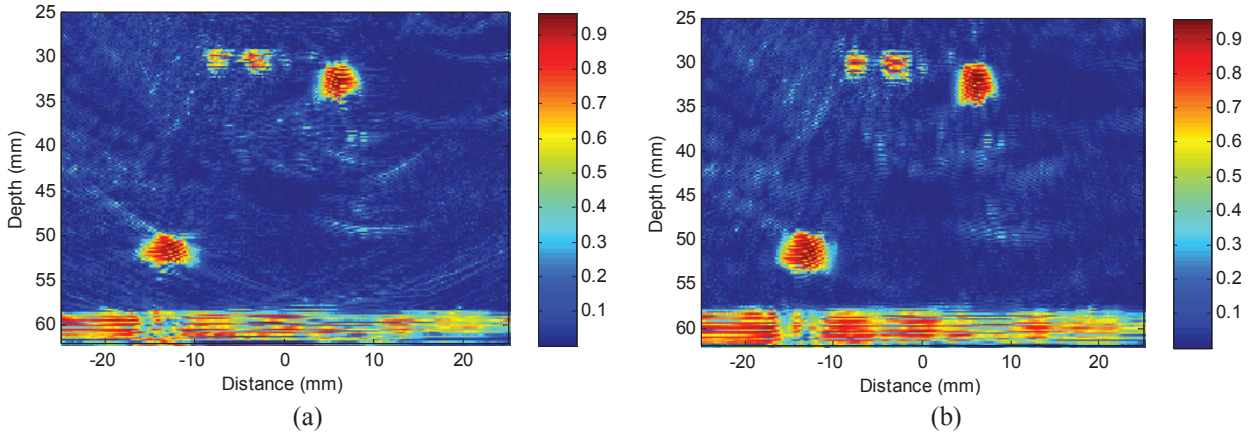

FIGURE 4. Coherence factors of mild steel block. (a) Computed with original data set, and (b) Computed with matched filtered data set.

Fig. 2(b) demonstrates the waveform at Element 68 processed with the optimised matched filter. Comparing to the original signal in Fig. 2(a), it seems that the target echoes are enhanced and the grain noise is reduced with matched filtering. The SNR is increased to 27 dB, and the matched filter observes 9 dB SNR gain for the A-scan signals. To form the image in Fig. 3(b), firstly, each A-scan waveform in the FMC data set is matched filtered, and

then the processed FMC data set is imaged with TFM. Comparing to the original TFM image in Fig. 3(a), it is evident that the clutter noise is further reduced, while all the legitimate reflectors are retained.

The Coherence Factors (CF) computed with the original FMC data set and the matched filtered data set are shown and compared in Fig. 4, with Fig. 4(a) the original data set and Fig. 4(b) the matched filtered data set. The Coherence Factor is described in the literature and defined as [17]

$$CF = \frac{\left|\sum_{n=1}^{N} x_n\right|^2}{N\sum_{n=1}^{N}\left|x_n\right|^2}, \tag{5}$$

where x_n is the received signal of channel n after proper receive focusing delays have been applied, and N is the number of array channels. The numerator represents the energy of the coherent sum obtained in conventional delay-and-sum beamforming, and the denominator represents the total incoherent energy that is N times the incoherent sum. The CF is a good index of focusing quality [17]. As can be seen from Fig. 4(a) and Fig. 4(b), the CFs corresponding to the side-drilled holes and the back-wall, especially to the two weaker reflectors located at a depth of 30 mm and a lateral position between -10 mm and 0, are greatly improved. It seems that the focusing quality by conventional delay-and-sum beamforming is improved when the matched filter is applied to each A-scan waveform individually in advance.

The matched filtering works in the temporal-spectral domain. A range of beamforming methods exploring the spatial diversity introduced by a transducer array were investigated in the literature, for example, the adaptive Capon beamformer [1], and thus there is a potential to combine these two categories of techniques as they work in different domains and may complement with each other. Fig. 3(c) shows the image obtained with the Capon beamformer using the matched filtered FMC data set. It is evident that the clutter noise is further reduced by exploiting both the temporal and spatial information.

Experiment II

A test sample made of INCONEL Alloy 617 with a thickness of around 150 mm is considered in this experiment. As described in the literature, Alloy 617 is a solid-solution, nickel-chromium-cobalt-molybdenum alloy with an exceptional combination of high-temperature strength and oxidation resistance, and it is readily formed and welded by conventional techniques [18]. Due to the attractive properties, Alloy 617 is widely used for components such as ducting, combustion cans, and transition liner in gas turbines as well as power-generating plants, both fossil-fuelled and nuclear.

The FMC data set is recorded at a sampling rate of 100 MHz, and each A-scan waveform is band-pass filtered to remove the DC drift and high frequency noise. The scenario is much more challenging than that in Experiment I, i.e. the grain size of Alloy 617 is much larger than mild steel, and the material is highly scattering to 5 MHz ultrasound, furthermore, the thickness is much larger, as a result, the grain noise is dominant and the SNR is pretty low.

Fig. 5(a) illustrates the image obtained with TFM using the band-pass filtered FMC data set in a dynamic range of 40 dB. The grain noise is quite significant and the back-wall reflection is weak. The image is very noisy and the back-wall is only partially visible at the depth of 147 mm. To form the image in Fig. 5(b), each A-scan waveform in the FMC data set is first processed with the optimised matched filter, and then the processed FMC data set is imaged with TFM. Comparing to the original TFM image in Fig. 5(a), it is evident that the grain noise is significantly reduced, and the back-wall reflection is enhanced in term of the strength as well as the visible lateral length.

To analyse the enhancement of focusing quality through optimal matched filtering, the coherence factors obtained with the original FMC data set and the matched filtered FMC data set are illustrated in Fig. 6(a) and Fig. 6(b), respectively. Fig. 6(a) demonstrates weak coherence testing everywhere even at the back-wall. As can be seen from Fig. 6(b), it is evident that the CFs corresponding to the back-wall are greatly enhanced, the maximum CF value is increased from 0.69 to 0.88, and much more points in the back-wall area show high CF values which make them distinct from the surrounding noise region. The CFs corresponding to the grain noise are somewhat reduced. It is clear that the quality of focusing with conventional delay-and-sum beamforming is significantly improved through matched filtering all A-scan waveforms, especially in this highly scattering material.

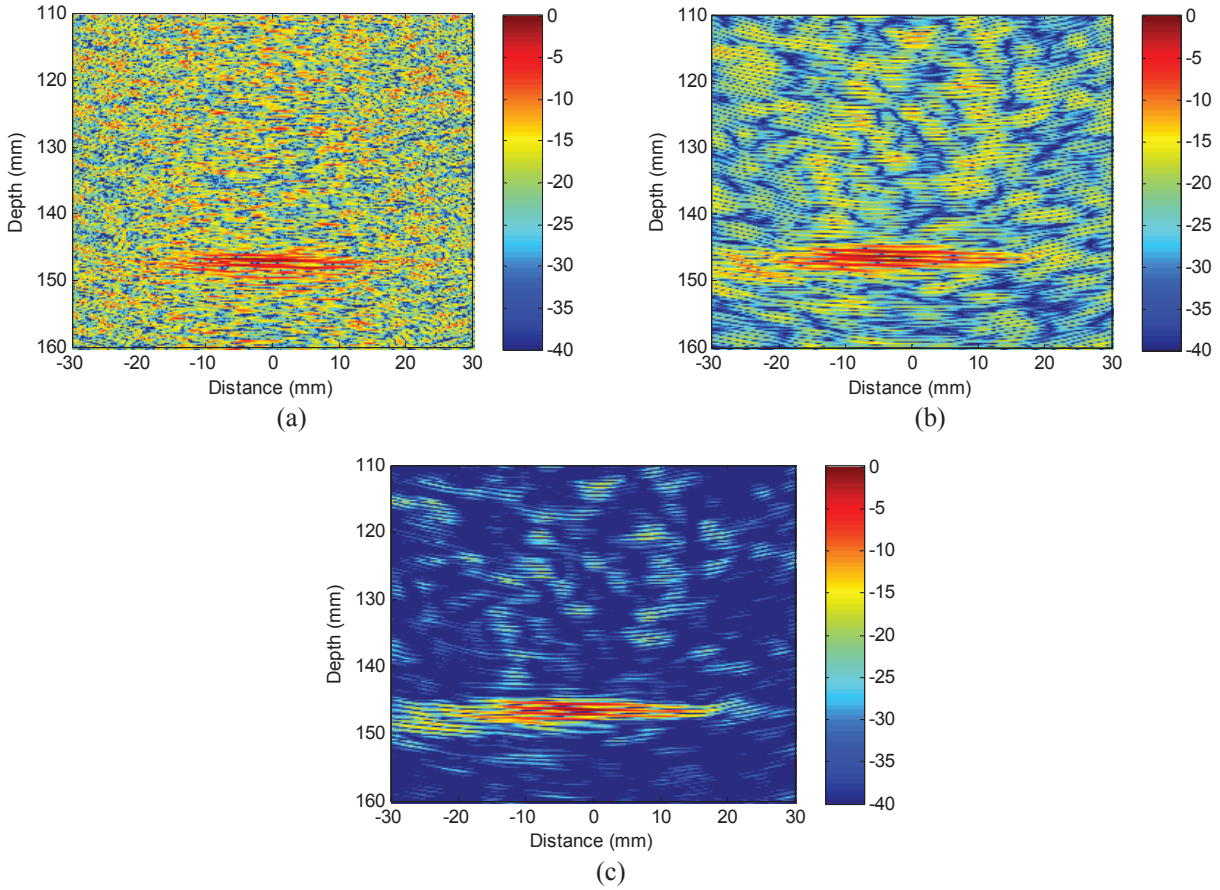

FIGURE 5. Images of INCONEL Alloy 617 sample. (a) TFM with original FMC data set, (b) TFM with matched filtered FMC data set, and (c) Adaptive beamforming with matched filtered FMC data set.

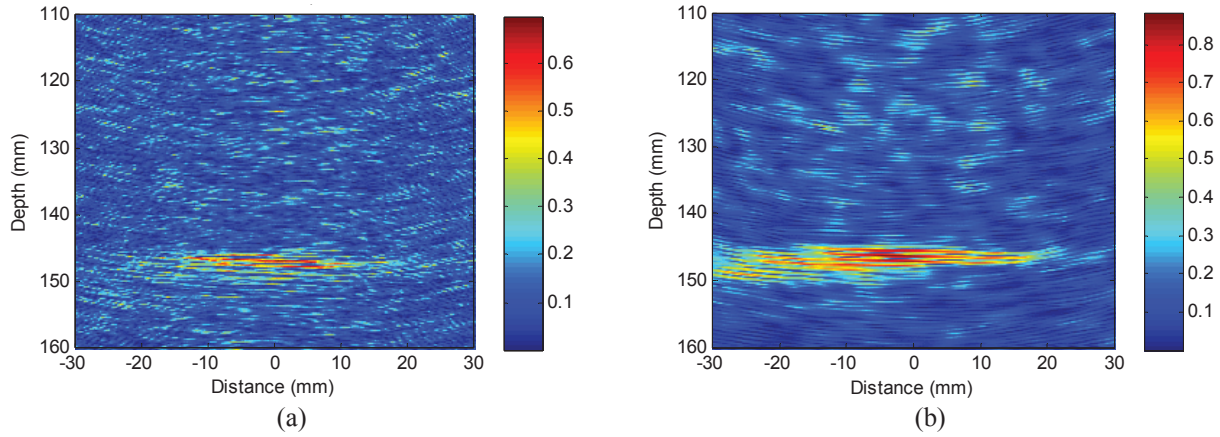

FIGURE 6. Coherence factors of INCONEL Alloy 617 sample. (a) Computed with original data set, and (b) Computed with matched filtered data set.

Fig. 5(c) demonstrates the image obtained with the adaptive beamformer using the matched filtered FMC data set. It is evident that the grain noise is further reduced while the back-wall reflection is greatly enhanced through

exploitation of both the temporal and spatial filtering. It seems that the matched filter and the adaptive beamformer are able to complement with each other to reduce the clutter noise.

CONCLUSIONS AND FUTURE WORK

In this paper, we present a novel approach for ultrasonic NDE of coarse grain materials using the optimized matched filters, which are designed to approximate the defect echoes. A particle swarm optimization (PSO) paradigm is employed to search for the optimal parameters in the filter response with an objective to maximize the output SNR. Experiments on samples made of mild steel and INCONEL Alloy 617 are conducted and the results confirm the advantages of the method. The benefits are obtained from two aspects: 1) the gain in SNR in A-scan waveforms through reducing grain noise and enhancing the target signals; and 2) the improvement on the focusing quality of the array, and the advantages become more significant if the grain size is coarser. The method offers a great potential to inspection and imaging of highly scattering materials, and applications to various industrial samples of alloys, stainless steel and composites are being investigated.

REFERENCES

1. M. Li and G. Hayward, "Ultrasound non-destructive evaluation (NDE) imaging with transducer arrays and adaptive processing," *Sensors* **12** (1) pp. 42-54, (2012).
2. M. Li, G. Hayward and B. He, "Adaptive array processing for ultrasonic non-destructive evaluation," *2011 IEEE International Ultrasonics Symposium (IUS) Proceedings*, (Orlando, FL, USA, October, 2011), pp. 2029-2032, (2011).
3. K. Ho, M. Li, R. O'Leary and A. Gachagan, "Application of frequency compounding to ultrasonic signals for the NDE of concrete," in *Review of Progress in Quantitative Nondestructive Evaluation*, eds. D. O. Thompson and D. E. Chimenti, (American Institute of Physics 1430, Melville, NY), **31**, pp. 1508-1515, (2012).
4. R. Gongzhang, M. Li, B. Xiao, T. Lardner and A. Gachagan, "Robust frequency diversity based algorithm for clutter noise reduction of ultrasonic signals using multiple sub-spectrum phase coherence," in *Review of Progress in Quantitative Nondestructive Evaluation*, eds. D. E. Chimenti, L, J. Bond and D. O. Thompson, (American Institute of Physics 1581, Melville, NY), **33**, pp. 1948-1955, (2014).
5. B. Xiao, M. Li, R. Gongzhang, R. O'Leary and A. Gachagan, "Image de-noising via spectral distribution similarity analysis for ultrasonic non-destructive evaluation," in *Review of Progress in Quantitative Nondestructive Evaluation*, eds. D. E. Chimenti, L, J. Bond and D. O. Thompson, (American Institute of Physics 1581, Melville, NY), **33**, pp. 1941-1947, (2014).
6. R. Gongzhang, M. Li, T. Lardner and A. Gachagan, "Robust defect detection in ultrasonic nondestructive evaluation (NDE) of difficult materials," *2012 IEEE International Ultrasonics Symposium (IUS) Proceedings*, (Dresden, Germany, October, 2012), pp. 467-470, (2012).
7. M. Li and G. Hayward, "A rapid approach to speckle noise reduction in ultrasonic non-destructive evaluation using matched filters," *2014 IEEE International Ultrasonics Symposium (IUS) Proceedings*, (Chicago, IL, USA, September, 2014), pp. 45-48, (2014).
8. K. Srinivasan, C. P. Chiou, and R. B. Thompson, "Ultrasonic flaw detection using signal matching techniques," in *Review of Progress in Quantitative Nondestructive Evaluation*, eds. D. O. Thompson and D. E. Chimenti, (Plenum Press, NY), **14**, pp. 711-718 (1995).
9. N. Ruiz-Reyes, P. Vera-Candeas, J. Curpian-Alonso, R. Mata-Campos, and J. C. Cuevas-Martinez, "New matching pursuit-based algorithm for SNR improvement in ultrasonic NDT," *NDT&E International* **38**(6) pp. 453-458 (2005).
10. R. Eberhart and J. Kennedy, "A new optimizer using particle swarm theory," *6th International Symposium on Micro Machine and Human Science Proceedings*, (Nagoya, Japan, October, 1995), pp.39-43, (1995).
11. M. Li and Y. Lu, "Improving the performance of GA-ML DOA estimator with a resampling scheme," *Signal Processing* **84** (10) pp. 1813-1822, (2004).

12. M. Li and Y. Lu, "Angle-of-arrival estimation for localization and communication in wireless networks,"*16th European Signal Processing Conference (EUSIPCO 2008) Proceedings*, (Lausanne, Switzerland, August 2008), pp. 1-5, (2008).
13. M. Li and Y. Lu, "Optimal direction finding in unknown noise environments using antenna arrays in wireless sensor networks," *7th International Conference on Intelligent Transportation Systems Telecommunications (ITST2007) Proceedings*, (Sophia Antipolis, France, June, 2007), pp. 332-337, (2007).
14. C. Holmes, B. Drinkwater and P. Wilcox, "Post-processing of the full matrix of ultrasonic transmit-receive array data for non-destructive evaluation," *NDT&E International* **38**(8), pp. 701-711, (2005).
15. M. Li and Y. Lu, "Maximum likelihood DOA estimation in unknown colored noise fields," *IEEE Transactions on Aerospace and Electronic Systems* **44** (3), pp. 1079-1090, (2008).
16. M. Li and Y. Lu, "Source bearing and steering-vector estimation using partially calibrated arrays," *IEEE Transactions on Aerospace and Electronic Systems* **45** (4), pp. 1361-1372, (2009).
17. P.-C. Li and M.-L. Li, "Adaptive imaging using the generalized coherence factor," *IEEE Transactions on Ultrasonics, Ferroelectrics, and Frequency Control* **50** (2), pp. 128-141, (2003).
18. INCONEL 617 Technical Data, http://www.hightempmetals.com/techdata/hitempInconel617data.php, accessed in July 2015.